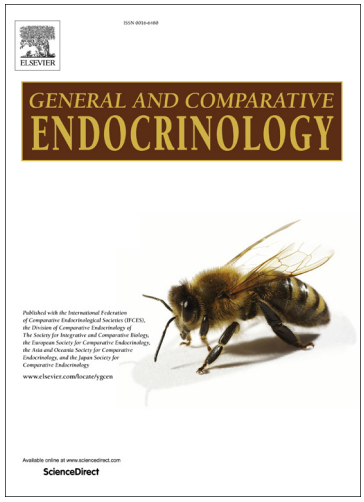

Genes and associated peptides involved with aestivation in a land snail

K.J. Adamson, T. Wang, B. Rotgans, T. Kruangkum, A.V. Kuballa, K.B. Storey, S.F. Cummins

PII: S0016-6480(15)30013-7
DOI: http://dx.doi.org/10.1016/j.ygcen.2015.10.013
Reference: YGCEN 12226

To appear in: *General and Comparative Endocrinology*

Received Date: 5 June 2015
Revised Date: 14 October 2015
Accepted Date: 19 October 2015

Please cite this article as: Adamson, K.J., Wang, T., Rotgans, B., Kruangkum, T., Kuballa, A.V., Storey, K.B., Cummins, S.F., Genes and associated peptides involved with aestivation in a land snail, *General and Comparative Endocrinology* (2015), doi: http://dx.doi.org/10.1016/j.ygcen.2015.10.013

Genes and associated peptides involved with aestivation in a land snail

K.J. Adamson[1], T. Wang[1], B. Rotgans[1], T. Kruangkum[1], A.V. Kuballa[1], K.B. Storey[2], S.F. Cummins[1]

[1] Genecology Research Centre, Faculty of Science, Health, Education and Engineering, University of the Sunshine Coast, Maroochydore DC, Queensland, Australia, 4558; [2] Institute of Biochemistry & Department of Biology, Carleton University, 1125 Colonel By Drive, Ottawa, ON, Canada K1S 5B6

[*]Corresponding author: Scott Cummins, scummins@usc.edu.au

Abstract

Some animals can undergo a remarkable transition from active normal life to a dormant state called aestivation; entry into this hypometabolic state ensures that life continues even during long periods of environmental hardship. In this study, we aimed to identify those central nervous system (CNS) peptides that may regulate metabolic suppression leading to aestivation in land snails. Mass spectral-based neuropeptidome analysis of the CNS comparing active and aestivating states, revealed 19 differentially produced peptides; 2 were upregulated in active animals and 17 were upregulated in aestivated animals. Of those, the buccalin neuropeptide was further investigated since there is existing evidence in molluscs that buccalin modulates physiology by muscle contraction. The *T. pisana* CNS contains two buccalin transcripts that encode precursor proteins that are capable of releasing numerous buccalin peptides. Of these, *Tpi-buccalin-2* is most highly expressed within our CNS transcriptome derived from multiple metabolic states. No significant difference was observed at the level of gene expression levels for *Tpi-buccalin-2* between active and aestivated animals, suggesting that regulation may reside at the level of post-translational control of peptide abundance. Spatial gene and peptide expression analysis of aestivated snail CNS demonstrated that buccalin-2 has widespread distribution within regions that control several physiological roles. In conclusion, we provide the first detailed molecular analysis of the peptides and associated genes that are related to hypometabolism in a gastropod snail known to undergo extended periods of aestivation.

Key words: Snail; *Theba pisana*; peptides; neuropeptides; aestivation; central nervous system

Background

Aestivation refers to a state of metabolic rate suppression (a dormant or resting state) during the summer or dry season, a state that is normally entered during times of restricted water or food, often during periods of extreme high summer temperatures (Storey and Storey, 2012). Both vertebrates and invertebrates use hypometabolism as a survival strategy; aestivating vertebrates include amphibians such as frogs (Hudson et al., 2008), toads (Armentrout and Rose, 1971) and salamanders (Barry and Shaffer, 1994), and reptiles such as lizards (Christian et al., 2003), crocodiles (Firth et al., 2010) and snakes (Winne et al., 2006). Aestivation among invertebrates has been well studied in pulmonate land snails (Storey, 2002) and also in some earthworms and insects (Bayley et al., 2010; Benoit, 2010) but other states that are highly comparable to aestivation (e.g. diapause in insects, dauer/diapause in nematodes) are also well studied (Hahn and Denlinger, 2011; Padilla and Ladage, 2012).

One of the challenges that aestivating animals encounter is to conserve water within the body, and this can be partially achieved by the animal sealing itself away from the environment. Snails typically elevate themselves to avoid higher temperatures at ground level or seek shelter in places such as crevices or under logs (Storey, 2002) while also sealing the operculum with an mucous epiphragm that greatly reduces water loss from the body. Regulated metabolic rate depression is also used to achieve a strong reduction in energy use that ensures longer lasting endogenous fuel reserves. Typically, aestivating animals show a reduction in metabolic rate to 5-40% of normal resting rate in the active state (Guppy and Withers, 1999). The mechanisms controlling metabolic rate depression must also be quickly reversible, since some species are known to become active within as little as 5 minutes after environmental conditions improve. Metabolic rate depression involves strongly reducing ATP turnover by coordinated reductions in both fuel catabolism and the rates of many ATP-expensive metabolic functions (e.g. ion channels, gene expression, protein synthesis, cell division). For example, in the aestivating land snail *Otala lactea*, activity of the membrane enzyme Na^+/K^+-ATPase, one of the biggest energy consumers in the cell, is reduced by 30% (Ramnanan and Storey, 2006; Storey and Storey, 2004). Indeed, ion channel activity (Na^+/K^+-ATPase, Ca^{2+}-calmodulin ATPase) and both initiation and elongation factors of protein synthesis (another major energy expenditure in cells) are strongly suppressed during aestivation via reversible protein phosphorylation (Ramnanan et al., 2009; Ramnanan and Storey, 2008; Storey and Storey, 2012). In addition, aestivation includes the specific implementation of cell protection measures via the selective up-regulation of some genes (e.g. chaperone proteins, antioxidant defenses) (Storey and Storey, 2012).

However, much remains to be learned about the gene expression and protein adaptation responses that support aestivation and/or regulate transitions to and from the aestivating state. To date, there have been very few gene/protein screening studies of aestivating species (Storey and Storey, 2010, 2012). Recent transcriptome sequencing projects have identified differential gene expression during aestivation in sea

cucumbers (*Apostichopus japonica*) and green-striped burrowing frogs (*Cyclorana alboguttata*) (Du et al., 2012; Reilly et al., 2013). In sea cucumbers, a comparison of transcripts from active and aestivating animals revealed 446 differentially expressed genes and, of these, 253 were down-regulated during aestivation and 193 were up-regulated; the functions of 34% of these genes are unknown (Du et al., 2012). In frogs, a comparison between active and 4-month estivating animals found differential up-regulation of genes associated with energy metabolism, antioxidant defence, cytoskeletal remodelling, and anti-apoptotic signalling during aestivation.

Peptides have been implicated in helicid snail hypometabolism. For instance, mass spectrometry has been used to determine changes in peptide profiles of the brain and haemolymph of the snail *Helix pomatia* during hibernation (Pirger et al., 2010). The output of selected peptides was increased or decreased in response to low temperatures. In the brain, 19 peptides/polypeptides were predominantly present in the active state, with 10 in the haemolymph. Other peptide/polypeptides (11 in the brain and 13 in the haemolymph) were present only in hibernation, while several peptides showed no difference between states. With such a diverse range of biological functions that need to be altered during hypometabolism, it is clear that some global control is necessary to not only regulate but also coordinate these changes, and little is known about this control.

The small white Italian snail, *Theba pisana,* is one of several snails native to the Mediterranean that are now established as pests in grain crops, pastures and vineyards in southern Australia (Baker, 1991, 2008; Baker, 1998). In Australia the snails are active during autumn, winter and spring, and aestivate in early summer as temperatures increase (Baker and Vogelzang, 1988). The central nervous system (CNS), hepatopancreas and foot muscle transcriptomes of *T. pisana* have been analysed, providing a summary of peptides (Adamson et al., 2015b). Of those, a total of 22 neuropeptides were found at significantly different levels in the CNS at activity compared to aestivation, including the small cardioactive peptide A (Adamson et al., 2015a).

In this study, we have performed a comprehensive molecular investigation of the responses of the CNS peptidome during *T. pisana* aestivation to confirm and help clarify precisely which extracellular neuropeptides (and their genes) are associated with regulating entry into and/or arousal from aestivation. We analyzed the CNS peptidome of *T. pisana* during active and aestivating states, finding 19 differentially expressed peptides. One of those peptides upregulated the buccalin, was further investigated at the gene and peptide level through gene and protein expression analyses.

Materials and Methods

Animals and tissue collection for proteome analysis

Mature *Theba pisana* were collected from agricultural sites surrounding Warooka, located on the Yorke Peninsula, South Australia in early spring (September). Snails were transported to the University of the Sunshine Coast (USC) and housed within purpose-built enclosures. Snails were provided with water and food (cucumber and carrot) *ad libitum* and maintained at room temperature.

Active snails were conditioned by feeding and supplied with water daily over 7 days. Snails to be used for aestivation experiments were placed into glass jars without food or water and kept in an incubator on a cycle of 12 h at 30°C with light, 12 h at 20°C dark, to emulate South Australian summer conditions. The positions of the snails were marked on the jars after 14 days. Any snails that had not moved following a further 21 days were deemed to be in aestivation.

Histology

Histological analysis was assessed to determine the cell structure of the circumesophageal nerve ring central nervous system (CNS) minus the buccal ganglia. Tissue samples that had been fixed in 4% paraformaldehyde were further dehydrated in ethanol before being embedded in a paraffin wax. The samples were then sectioned in serial transverse cross sections using a rotary microtome and stained with Harris's hematoxylin and eosin stains. The slides were permanently mounted using DePex (BDH Chemicals). The sections were viewed and photographed with a light microscope (BX51; Olympus) equipped with a camera system (UC50; Olympus).

Protein isolation from CNS and nanoHPLC-ESI-Triple TOF peptide identification and label-free quantification

Both active moving and aestivated *T. pisana*, were killed by immersion in liquid nitrogen prior to CNS removal. CNS were then separately pooled before immediate re-freezing in liquid nitrogen prior to storage at -80°C until use. Frozen samples of CNS were ground to a powder under liquid nitrogen in a mortar, then quickly weighed while frozen and homogenized in extraction buffer (90% methanol, 9% glacial acetic acid in deionized water) in a 1:5 w:v ratio. Crude extracts were then sonicated with three pulses, 30 s each, and centrifuged for 20 min (16,000 x g, 4°C). Supernatant was collected and lyophilised.

The CNS extracts were analyzed by LC-MS/MS on a Shimadzu Prominance Nano HPLC (Japan) coupled to a Triple-ToF 5600 mass spectrometer (ABSCIEX, Canada) equipped with a nano electrospray ion source. Aliquots (6 µL) of each extract were injected onto a 50 mm x 300 µm C18 trap column (Agilent Technologies, Australia) at 30 µL/min. The samples were de-salted on the trap column for 5 minutes using solvent A [0.1% formic acid (aq)] at 30 µL/min. The trap column was then placed in-line with the analytical

nano HPLC column, a 150 mm x 75 µm 300SBC18, 3.5 µm (Agilent Technologies) for mass spectrometry analysis. Peptide elution used a linear gradient of 1-40% solvent B [90:10 acetonitrile:0.1% formic acid (aq)] over 35 min at 300 nL/minute flow rate, followed by a steeper gradient from 40% to 80% solvent B over 5 min. Solvent B was then held at 80% for 5 min to wash the column and then returned to 1% solvent B for equilibration prior to the next sample injection. The ionspray voltage was set to 2400V, declustering potential (DP) 100V, curtain gas flow 25, nebuliser gas 1 (GS1) 12 and interface heater at 150^{o}C. The mass spectrometer acquired 500 ms full scan TOF-MS data followed by 20 by 50 ms full scan product ion data in an Information Dependent Acquisition (IDA) mode. Full scan TOFMS data was acquired over the mass range 350-1800 and for product ion ms/ms 100-1800. Ions observed in the TOF-MS scan exceeding a threshold of 100 counts and a charge state of +2 to +5 were set to trigger the acquisition of product ion, ms/ms spectra of the resultant 20 most intense ions. The data was acquired and processed using Analyst TF 1.5.1 software (ABSCIEX, Canada).

Proteins were identified by database searching using PEAKS v7.0 (BSI, Canada) against the protein database built from the CNS transcriptome (Adamson et al., 2015b). Search parameters were as follows: no enzyme was used; variable modifications included methionine oxidation, conversion of glutamine to pyroglutamic acid, deamidation of asparagine and amidation. Precursor mass error tolerance was set to 20 ppm and a fragment ion mass error tolerance was set to 0.05 Da. Maximum expectation value for accepting individual peptide ion scores [-10*Log(p)] was set to ≤0.01, where p is the probability that the observed match is a random event. Proteins and their supporting peptides were obtained and analysed. The quantitative analysis of proteins was carried out using the label-free quantification module (PEAKS Q) of PEAKS v7.0, and relative concentrations of proteins at two stages were compared. Biological triplicates [i.e., (A1, B1), (A2, B2) and (A3, B3)] of each stage were used in tandem repeats, and the average values were calculated as the final results. Extracted peptides were quantified based on absorbance at 280 nm using a NanoDrop spectrophotometer for later normalization. For each run, about 1.5 µg of the mix was then analyzed via liquid chromatography combined with mass spectrometry on a Triple-TOF. In addition to the protein identification method mentioned above, peptide feature fold change and protein unique peptide were set to 2, peptide feature significance filter was set to 0.01 and other parameters were adjusted according to the 'volcano plot' generated by PEAKS.

Gene analysis

To characterize which of the significantly up- and down-regulated CNS peptides identified from MS/MS corresponded to protein precursors, a BLAST analysis was performed against an in-house derived *Theba pisana* protein database (http://thebadb.bioinfo-minzhao.org/). Schematic diagrams of protein domain structures were prepared using Domain Graph (DOG, version 2.0) software (Ren et al., 2009) . Buccalin-like

sequences were derived by BLASTp analysis of the NCBI database, then protein sequences were aligned using the MEGA 5.1(Tamura et al., 2011) platform with the clustalW protocol utilising the Gonnet protein weight matrix. Neighbour-joining trees were generated based on these alignments. Gene expression levels were determined from RNA-seq data (NCBI Genbank under SRA file SRP056280) using the FPKM method, which represents the fragments per kilobase of transcript per million fragments mapped.

Absolute qPCR

RNA was extracted from tissue using TRIzol Reagent (Invitrogen), as per the manufacturer's protocol. Each sample contained CNS from 3 *T. pisana*. A total of 15 aestivating and 14 active snail samples were prepared. Following extraction, RNA was assessed for quality by visualisation on a 1.2% denaturing formaldehyde agarose gel, and quantified using a Nanodrop spectrophotometer (Thermo Scientific). Approximately 500 ng of total RNA were reverse-transcribed using QuantiTect Reverse Transcription kit (Qiagen) as per the manufacturer's protocol. Products were visualised by agarose gel electrophoresis, then cDNA was stored at -20°C until use.

Absolute qPCR was performed using a SensiFast HRM kit (Bioline) as per the manufacturer's protocol, on a Rotor-gene 6000 cycler (Corbett research) using Rotor-gene 1.7.87 software. A total volume of 10 µl per reaction containing 1x SensiFast, and 400 nM of each primer, with 1 µl of template cDNA. All reactions, including a no template control (NTC) for each primer pair, were done in duplicate.

Cycling parameters were: an initial hold at 95°C for 2 min followed by 40 cycles of denaturation at 95°C for 5 s, annealing at 60°C for 10 s and extension at 72°C for 20 s acquiring to cycle A (Green). Melt curve analysis was performed rising by 1°C per cycle from 70°C to 95°C and was held for 90 s on the first step and 5 s on subsequent steps. Quantitative PCR primers for the gene of interest (*Tpi-buccalin-2*) were designed from transcriptome sequences using Primer3 software. Primers were sourced from Genworks and checked via PCR. A standard curve of known concentration was prepared for the gene of interest (*Tpi-buccalin*). Complementary DNA was amplified using the primers forward ACAGCCGAGCCCATATACAC, reverse GCGATGCTCCAGAATAAAGC and the PCR products were used as template for the standard curves. Following PCR the amplified products were visualised to check for correct size and then purified using the QIAquick kit (Qiagen). Purified products were quantified three times and mean concentrations calculated. From this and the known length of the products, the copy number was calculated using the calculator of URI Genomics & Sequencing Centre (http://www.uri.edu/research/gsc/resources.cdna.html). A DNA concentration of 2 x 10^9 was then prepared and serially diluted six times into 1:10 dilutions. A standard curve for the gene using the serially diluted PCR product was prepared (in triplicate) using the reaction conditions described above. No template control (NTC) was carried out in duplicate. Target gene expression levels of the CNS tissue from active and

aestivating animals was quantified using the qPCR described above, samples were run in duplicate using cDNA synthesised from CNS RNA.

In situ hybridization

The *T. pisana* buccalin-2 open reading frame was cloned into a pUC plasmid (Genscript). Sense and antisense digoxigenin (DIG)-labelled riboprobes were prepared using a DIG RNA labelling mix kit (Roche) as per protocol (Cummins et al., 2011), using SP6 and T7 polymerase (SP6 5'-TAATACGACTCACTATAGGG -3', T7 5'-ATTTAGGTGACACTATAG3'). *T. pisana* CNS derived from active and aestivated snails was fixed in 4% paraformaldehyde overnight at 4°C and stored in 70% ethanol, before dehydration in ascending concentrations of ethyl alcohol for 30 min each, cleared in xylene three times, infiltrated, and embedded in paraffin. Serial transverse sections of the tissues were cut at 5 µm thickness using a microtome. Sections were then deparaffinized in xylene and rehydrated in a descending concentration of ethanol. Sections were then washed and rehydrated into phosphate buffered saline (PBS) with 0.1% Tween 20. Sections were pre-hybridised for 3 hours in prehybridisation solution [50% formamide, 5x sodium saline citrate, 5 mM EDTA, 1% Denhardt´s solution (Sigma), 100 µg/ml heparin, 100 µg/ml tRNA, 0.1% Tween20] at 55°C. Hybridisation was performed using the same solution but adding 200 ng/ml DIG-labelled riboprobe overnight at 42°C. Washing, detection and mounting for viewing was performed as described by Cummins et al. (Cummins et al., 2011). Sections were viewed under a confocal laser-scanning microscope (Nikon).

Immunolocalisation

Rabbit polyclonal antibodies were generated to the Tpi-buccalin-2 precursor by Genscript using keyhole limpet hemocyanin-coupled peptides-RLDKFGFSGGI-amide. CNS was isolated from active and aestivated *T. pisana* then fixed in 4% paraformaldehyde overnight at 4°C, before dehydration in ascending concentrations of ethyl alcohol for 30 min each, cleared in xylene three times, infiltrated, and embedded in paraffin. Serial transverse sections of the tissues were cut at 5 µm thickness using a microtome. Sections were then deparaffinized in xylene and rehydrated in a descending concentration of ethanol. Subsequently, sections were incubated in 0.1% glycine in 0.1 M PBS for 30 min, and washed three times with PBS with 0.1 M PBS containing 0.4% Triton X-100 (PBST). Non-specific binding was blocked in 4% normal goat serum in PBST for 2 h, followed by incubation in the primary antibody (anti-peptide) at an optimal dilution of 1:1000 in blocking solution, at 4^{o}C overnight. Sections were then washed 3 times with PBST, and incubated for 2 h with Alexa Fluor 488 conjugated goat anti-rabbit IgG (Santa Cruz, USA) at room temperature. After washing with PBST, nuclei were stained with DAPI (Santa Cruz, USA) for 10 min. Finally, sections were washed with PBST and mounted with VECTA shield fluorescent mounting medium (Molecular Probes) before viewing under a confocal laser-scanning microscope (Nikon). In negative

controls, tissues were processed by the same protocol, but preimmune mouse serum was used instead of primary antibody.

Results and Discussion

Previous investigation of the *T. pisana* CNS transcriptome revealed that this snail may contain as many as 5504 precursor proteins that are destined to secrete peptides. Of these, full-length precursors were identified in *T. pisana* for 35 known molluscan neuropeptides (Adamson et al., 2015b). In this study, we were most interested in identifying which of those neuropeptides may be associated with the aestivation process.

Histology of the Theba pisana *CNS*

Prior to obtaining the aestivation-associated CNS peptides, it was important to explore the anatomical and histological make-up of the *T. pisana* CNS. To achieve this, the CNS was removed for light microscopic (**Figure 1A**) and hematoxylin/eosin histological examination (**Figure 1B** and **Figure S1**). The cerebral ganglia in *Theba* are located above the esophagus, and consist of a left and right ganglion, connected by a cerebral commissure. These ganglion are divided into 3 regions; the procerebrum, the mesocerebrum and the metacerebrum. Major nerve cords connect the cerebral ganglia to the subesophageal ganglia, including pairs of pedal, pleural and parietal ganglia, and a single visceral ganglion. This general organisation is consistent with that found in other land snails, including *Cornu* and *Achatina*, and the pulmonate freshwater snail *Lymnaea*, with a ring of ganglia circling the esophagus and inclusive of multiple ganglia (Chase, 2000; Chase and Tolloczko, 1993). While the area of the body for which each ganglia control in molluscs are generally accepted, it appears that there are often multiple ganglia involved in functions that regulate various metabolic events, such as breathing (Syed et al., 1990) and heart rate (Arshavsky et al., 1990). A summary schematic of the *T. pisana* CNS is shown in **Figure 1C**.

Identification of differentially expressed peptides in active and aestivated Theba pisana *CNS*

Peptide extraction of the CNS followed by LC-MS analysis was used to identify those peptides present in the *T. pisana* CNS, then we proceeded to identify those differentially expressed between active and aestivating snails. A general workflow for this analysis is shown in **Figure 2**. To ensure that aestivated snails did not begin arousal, so that CNS samples accurately reflected the natural deep aestivation state, snails were rapidly killed by immersion in liquid nitrogen prior to CNS removal. Active snails were also rapidly killed with liquid nitrogen, an approach that had not been implemented in our prior analysis of aestivation peptides in the *T. pisana* CNS (Adamson et al., 2015a). We identified 19 peptides that were

differentially expressed, including 8 that contain a C-terminal amide (**Figure 3, Table 1** and **File S1**). Those CNS peptides that have not previously been characterised were termed Aestivation-associated peptides (AAPs). Of the 19 peptides differentially expressed, only two peptides were up-regulated in active snails. One of these (AAP14) corresponds to a precursor protein that has not been previously identified in any species, while the other is Leu-Phe-Arg-Phe (LFRF). The remaining 17 peptides were up-regulated in aestivating snails, including the molluscan neuropeptides for *T. pisana* small cardioactive peptide (sCAP), feeding circuit-activating peptide (FCAP), enterin, pleurin, sensorin-A, a LASGLV-like peptide and buccalin.

T. pisana sCAP, FCAP, enterin, pleurin and sensorin-A have been investigated in some aquatic molluscs. The sCAP was first identified in the marine slug *Aplysia* where it appears to be highly concentrated in the buccal ganglia, implying an important role in feeding. Besides the buccal ganglia, it is also present in fibres and neuronal bodies throughout the CNS, suggesting its involvement in more widespread functions (Lloyd et al., 1985). *T. pisana* contains 3 sCAP precursor isoforms, each containing an $sCAP_A$ peptide (Adamson et al., 2015a). In our study, we found that Tpi-FCAP was exclusive to the CNS of aestivating snails with none detected in active snails (**Figure 3** and **Table 1**). FCAP was also initially identified in *Aplysia*, where it was implicated in the regulation of feeding. Similar to sCAP, this peptide is distributed throughout various areas of the CNS, suggesting multiple functions (Sweedler et al., 2002). The peptide enterin, also recognised as a feeding-associated neuropeptide in *Aplysia*, is found throughout its CNS, indicating involvement in functions other than feeding (Furukawa et al., 2001).

The peptide pleurin has previously been identified in *Lottia* and in *Aplysia*, where the precursor is found in the right pleural ganglion (Moroz et al., 2006; Veenstra, 2010). The sensorin-A peptide has also been found in the cerebral and buccal ganglia of *Aplysia* (Brunet et al., 1991), and in one neuron of each pedal ganglion of *Lymnaea* (Steffensen et al., 1995). An extensive *in silico* analysis of *Pinctata fucata* and *Crassostrea gigas* failed to identify pleurin and sensorin homologs, suggesting they have been lost in bivalve molluscs (Stewart et al., 2014). Furthermore, we identified a peptide cleaved from the LFRF precursor that appears to be down-regulated in the *T. pisana* CNS during aestivation (**Table 1**); this peptide precursor contains the sequence SDSAQNPMDNEEE and includes 6 LFRF-like peptides. This peptide is not present in other mollusc LFRF precursors and has not been functionally characterised. A LASGLV-like precursor with 13 predicted cleavage peptides, including 6 copies of RPFDELGSG which is up-regulated in aestivation is highly conserved in *Aplysia californica,* within a predicted buccalin-like peptide precursor, however there is little overall similarity to buccalin. The majority of the remaining peptides identified as differentially expressed, besides buccalin (**Figure 3** and **Table 1**), match to precursor sequences that resemble either uncharacterised peptides or unknown proteins.

We identified 5 different buccalin peptides that are cleaved from two *T. pisana* buccalin precursor proteins and are up-regulated during snail aestivation (**Figure 3** and **Table 1**), corresponding to Tpi-buccalin-1 and Tpi-buccalin-2. Our initial *in silico* screen for neuropeptides within the *T. pisana* CNS had not revealed these buccalin precursors (Adamson et al., 2015a), possibly due to divergence with other species buccalin. The neuropeptide buccalin was first described in the buccal ganglia of *Aplysia* where it was shown to decrease the number of muscle contractions in the accessory radula closer, used during biting (Cropper et al., 1988). Since then, the closely related neuropeptides, buccalin B and buccalin C, were noted to be more effective (2-3x) at depressing radula contractions (Miller et al., 1993; Vilim et al., 1994; Weiss et al., 1988). Similar to Tpi-buccalins, the *Aplysia* buccalins contain multiple identical peptide repeats; for example, the buccalin C peptide is cleaved from a precursor containing a total of 19 buccalin-related peptides (Miller et al., 1993). There is evidence that buccalin is not only involved in *Aplysia* feeding, but also in functions controlled by the central ganglia, including cerebral and pleural ganglia (Miller et al., 1992; Raymond et al., 1989; Rosen et al., 1989). In other molluscs, little functional knowledge has been obtained for buccalin, although we do know that in *L. stagnalis,* it is primarily found in the pedal and buccal ganglia, ganglia that regulate feeding and locomotion. Smaller numbers of buccalin neurons were found in the cerebral, right parietal and visceral ganglia (Santama et al., 1994).

Besides *Aplysia* and *Lymnaea*, buccalin precursor genes have been found in a variety of other molluscs through *in silico* genome or transcriptome mining, including those from *Lottia gigantea* (Veenstra, 2010), *C. gigas* (Stewart et al., 2014), and *Biomphalaria glabrata* (Lockyer et al., 2007). Such *in silico* analyses can only predict that a bioactive peptide is produced, yet alternative splicing events may produce overlapping sets of peptides (Buck et al., 1987; Weiss et al., 1989). In the pelagic sea slug *Clione limacine,* buccalin was detected in all central ganglia except the pleural ganglia using an *Aplysia* buccalin A antibody (Norekian and Satterlie, 1997).

Since buccalin has an obvious role in the regulation of muscle contraction in the aquatic molluscs, as well as noted widespread distribution throughout the CNS, we speculated that the buccalin peptide could regulate metabolic events in aestivating snails. For that reason, Tpi-buccalin was further investigated via transcriptome screening and comparative sequence analysis, followed by spatial expression analysis. Of the buccalins identified, the *Tpi-buccalin-2* transcript and associated up-regulated peptide was targeted since its relative expression profile in the CNS far exceeded that of other buccalin isoforms (Adamson et al., 2015b). In fact, *Tpi-buccalin-2* appears to be one of the most highly expressed transcripts within the CNS (combined active and aestivated adult animals; FPKM= 2785), with expression relatively low in hepatopancreas (FPKM=1.59) and muscle (FPKM=8.3). *Tpi-buccalin-1* had relatively low levels of expression in all tissues (FPKM <10) (**Table 2**).

Schematics are presented in **Figure 4A** showing the organisation of Tpi-buccalin precursors and their comparison with known buccalin precursors from other species. Some features of interest include; Tpi-buccalin-like repeats vary from 10-11, depending on the precursor. From both buccalin precursors there are a total of 19 unique buccalin-like peptides and of these only 3 have more than 1 copy per precursor (**Table 1**). Other molluscan buccalin precursors contain a similar general organisation, although *L. gigantea* and *A. californica* show a greater number of buccalin-like peptides (**Figure 4A**).

A multiple sequence alignment of the four Tpi-buccalin precursors shows conservation between Tpi-buccalin-1 and Tpi-buccalin-2 within the predicted active peptides (**Figure 4B**). Based on our MS/MS data, only 1 of the buccalins showed post-translational amidation, ELDPYGFSARIamide, however peptide amidation has been shown in most cases to be essential for bioactivity (Clarke et al., 2008; Merkler, 1994). Phylogenetic tree analysis demonstrates that Tpi-buccalin-1 clusters most closely to the identified buccalin from *Cornu aspersum* (**Figure 4C**). Helicid buccalins appear to cluster more closely with bivalve buccalin, rather than the other gastropods represented, *L. gigantea* and *A. californica*.

Absolute qPCR was performed on CNS samples from active and aestivated snails to determine relative gene expression of the *Tpi-buccalin-2* precursor. While there was a trend for this gene to be up-regulated in CNS of aestivated snails, this was not statistically significant [Student t-test P(T<=t) two-tail 0.064894; **Figure 4D**]. This lack of differential gene expression indicates that the bioactive form of this neuropeptide is up-regulated in aestivation through some means other than an increase in gene expression, possibly via some form of post-translational modification of the peptide (Mann and Jensen, 2003). Alternatively, buccalins may simply accumulate and be stored within neuron secretory vesicles during aestivation but not utilized until the snail returns to normal activity. For example, in gastropods there are neuropeptides known that are produced and stored within cell secretory vesicles, as demonstrated in *Aplysia* bag cell neurons (Fisher et al., 1988). The neuropeptide egg-laying hormone (ELH) is produced during periods of inactivity, in preparation for reproduction-associated egg laying. Upon stimulation of the bag cells via another neuropeptide, ELH is secreted into the hemolymph. Also, several bioactive peptides appear at greater immunoreactive intensity within the cerebral ganglia of hibernating *C. apersa*, likely a result of accumulation during inactivity (Bernocchi et al., 1998). Similarly, the bucculin precursor is likely transcribed and post-translationally processed into its multiple peptides and stored within secretory vesicles, awaiting an unknown trigger for release. This could be beneficial considering the rapid speed with which *Theba* reanimates to full activity (~ 5 min, personal observation) and also to help conserve energy that would otherwise be required for protein synthesis. A role in modulation of acetylcholine release would ultimately impact on muscle excitability.

Other possibilities could include increased stability (ie. decreased turn-over) of the mRNA under aestivating conditions or a mechanism that confers preferential translation of the transcript versus the

majority of transcripts that are suppressed either by (a) reduced gene transcription or (b) mRNA storage into stress granules during hypometabolism, or (c) a sequence that allows preferential translation by ribosomes during hypometabolism. For example, end-dependent translation can be strongly suppressed in hypometabolic or stressed states but mRNAs that have internal ribosome entry sites are translated when translation of most mRNAs is repressed (Hellen and Sarnow, 2001; Johannes and Sarnow, 1998) – e.g. most chaperones have this as well as various transcription factors that mediate the "stress response".

Temporal and spatial expression of Tpi-buccalin-2 in the CNS

In situ hybridisation was employed to investigate spatial gene expression in the CNS tissue using a *Tpi-buccalin-2*-specific DIG-labeled riboprobe. Since we had identified no significant difference in expression of mRNA levels between active and aestivated snails using qPCR, we analysed gene expression at only one metabolic state, aestivation. Negative controls using a sense riboprobe indicated little or no staining throughout the CNS (**Figure 5A**). This result implied an absence of non-specific binding in the target tissue. Antisense riboprobes showed staining in several areas of the CNS, including the cerebral ganglia (**Figure 5B, C**), and the cerebral-pleural connective nerve (**Figure 5B, D**). Two areas of expression appeared specifically within nerve fibres (**Figure 5B, E, F**). A high level of gene expression was observed in the region of the visceral ganglia (**Figure 5B, G**).

The Tpi-buccalin-2 peptide R_{102}LDKFGFSGGI-amide was identified as being up-regulated during aestivation. This buccalin is not present in the other isoforms, although it may have similarity at the both the primary and structural level to some other buccalin peptides. A polyclonal antibody was generated to this peptide for spatial immunolocalization within the CNS of aestivated *T. pisana.* We found that this neuropeptide was widely distributed throughout the CNS of aestivated and active snails **(Figure 6)**. Expression can be observed within regions of the cerebral ganglia, pleural ganglia, parietal ganglia, pedal ganglia and visceral ganglia **(Figure 6A-L).** Within the cerebral ganglia, immunopositive staining is clearly observed within the metacerebrum and cerebral-pleural connective fibre (**Figure 6A,B,D,E,F,K).** Individual neurons were observed within the regions of pleural-parietal-pedal **(Figure 6A,C,G,I)** and in close association (**Figure 6J,L**). Two individual immunoreactive neurons can be seen in the visceral ganglia region of the CNS **(Figure 6G,H)**. No significant differences in spatial peptide expression were observed between active and aestivated CNS using this method (**Figure S2, S3**). Isotopic hybridization methods are generally considered to be more sensitive for detecting expression, thus would be more amenable to quantitative spatial analysis.

High levels of Tpi-buccalin in the cerebral ganglia, and the subesophageal ganglia are consistent with the widespread buccalin distribution observed in other molluscs (Miller et al., 1992; Raymond et al.,

1989; Rosen et al., 1989). Based on the spatial expression of Tpi-buccalin-2 transcript and peptide within regions of the CNS, we may speculate upon certain physiological functions it may regulate. Within the cerebral ganglia of snails, the procerebrum region controls olfactory function, the mesocerebrum controls reproduction and the metacerebrum regulates motor actions (Chase and Tolloczko, 1993). Within the pleural-parietal-visceral-pedal, the pairs of pedal control the foot, the pleural controls the mantle, parietal controls the pallial cavity, and a single visceral ganglia regulates the visceral organs (Chase and Tolloczko, 1993). Buccalin expression within these various ganglia implicates it in activities controlled by those ganglia. In the land snails studied, the visceral ganglia is known to regulate the heart (Chase, 2000), thus, the presence of buccalin within this region is consistent with a functional role in controlling heart rate, which is known to slow dramatically during aestivation (Storey and Storey, 1990). Similarly, relatively high concentrations of several bioactive peptides in the mesocerebrum of hibernating *C. aspersum*, could be regulating mating and avoidance behaviour upon reactivation (Bernocchi et al., 1998). Therefore, the widespread distribution of Tpi-buccalin probably reflects the diversity of functions of buccalin, including the regulation of muscle contractions in the heart (visceral ganglia) and in breathing (pleural ganglia). Further work would be required to determine exactly how many buccalin-expressing neurons are present and their location within the various ganglia. In addition, it would be of interest to precisely assess buccalin concentration within individual neurons during aestivation and normal activity.

Conclusions

In summary, we have performed a comprehensive molecular investigation of CNS peptides associated with aestivation by comparative mass spectral analysis, followed by spatial gene and peptide expression of the Tpi-buccalin. We speculate that increased levels of Tpi-buccalin, and other peptides identified during aestivation, relate to accumulation within CNS neurons. When released, this peptide may modify the animal's physiological response (e.g. muscle contraction strength or rate) that occurs in the aestivating to active transition (or is needed in a sustained manner in the active state). This work sets a foundation to clarify precisely what are the genes and extracellular peptides that trigger hypometabolism and maintains aestivation in land snails, and possibly other molluscs.

Abbreviations

CNS: central nervous system; FPKM: Fragments per kilobase of exon region in a given gene per million mapped fragments; GDH: glutamate dehydrogenase; GO: gene ontology; MS: mass spectrometry; FCAP: feeding circuit-activating peptide; sCAP: small cardioactive peptide.

Competing interests

The authors declare that they have no competing interests.

Author's contributions

KJA carried out the experimental analysis, constructed figures, tables and drafted the manuscript. BAR prepared immunocytochemical tissues. TW carried out mass spectral proteome work. TK helped to perform the histological reconstruction of the animal CNS. AVK, KBS and SFC conceived the idea and obtained funding for the experiments and drafted the manuscript. All authors read and approved the final manuscript.

Acknowledgements

This work was supported by grants from the Australian Research Council (KBS, SFC) and the Grains Research Development Corporation (KA). We thank Dr Alun Jones (Institute for Molecular Bioscience, the University of Queensland) for advice and assistance with the tandem mass spectrometry. This research was undertaken with the assistance of resources from the National Computational Infrastructure (NCI), which is supported by the Australian Government.

References

Adamson, K.J., Wang, T., Rotgans, B., Kuballa, A.V., Storey, K.B., Cummins, S.F., 2015a. Differential peptide expression in the central nervous system of the land snail *Theba pisana*, between active and aestivated. Peptides.

Adamson, K.J., Wang, T., Zhao, M., Bell, F., Kuballa, A.V., Storey, K.B., Cummins, S.F., 2015b. Molecular insights into land snail neuropeptides through transcriptome and comparative gene analysis. BMC genomics 16, 308.

Armentrout, D., Rose, F.L., 1971. Some physiological responses to anoxia in the great plains toad, *Bufo cognatus* Comparative Biochemistry and Physiology Part A: Physiology 39, 447-455.

Arshavsky, Y.I., Deliagina, T., Gelfand, I., Orlovsky, G., Panchin, Y.V., Pavlova, G., Popova, L., 1990. Neural control of heart beat in the pteropod mollusc *Clione limacina*: coordination of circulatory and locomotor systems. Journal of Experimental Biology 148, 461-475.

Baker, G., 1991. Production of eggs and young snails by adult *Theba pisana* (Muller) and *Cernuella virgata* (Da Costa) (Mollusca, Helicidae) in laboratory cultures and field populations. Australian Journal of Zoology 39, 673-679.

Baker, G., 2008. The population dynamics of the mediterranean snails *Cernuella virgata, Cochlicella acuta* (Hygromiidae) and *Theba pisana* (Helicidae) in pasture–cereal rotations in South Australia: a 20-year study. Animal Production Science 48, 1514-1522.

Baker, G., Vogelzang, B., 1988. Life history, population dynamics and polymorphism of *Theba pisana* (Mollusca: Helicidae) in Australia. Journal of Applied Ecology, 867-887.

Baker, G.H., 1998. Recognising and responding to the influences of agriculture and other land-use practices on soil fauna in Australia. Applied Soil Ecology 9, 303-310.

Barry, S.J., Shaffer, H.B., 1994. The status of the California tiger salamander (*Ambystoma californiense*) at Lagunita: A 50-year update. Journal of Herpetology, 159-164.

Bayley, M., Overgaard, J., Hoj, A.S., Malmendal, A., Nielsen, N.C., Holmstrup, M., Wang, T., 2010. Metabolic changes during estivation in the common earthworm *Aporrectodea caliginosa*. Physiological and Biochemical Zoology 83, 541-550.

Benoit, J.B., 2010. Water management by dormant insects: comparisons between dehydration resistance during summer aestivation and winter diapause. Prog Mol Subcell Biol 49, 209-229.

Bernocchi, G., Vignola, C., Scherini, E., Necchi, D., Pisu, M., 1998. Bioactive peptides and serotonin immunocytochemistry in the cerebral ganglia of hibernating *Helix aspersa*. Journal of Experimental Zoology 280, 354-367.

Brunet, J.-F., Shapiro, E., Foster, S.A., Kandel, E.R., Iino, Y., 1991. Identification of a peptide specific for *Aplysia* sensory neurons by PCR-based differential screening. Science 252, 856-859.

Buck, L.B., Bigelow, J.M., Axel, R., 1987. Alternative splicing in individual *Aplysia* neurons generates neuropeptide diversity. Cell 51, 127-133.

Chase, R., 2000. Structure and function in the cerebral ganglion. Microscopy research and technique 49, 511-520.

Chase, R., Tolloczko, B., 1993. Tracing neural pathways in snail olfaction: from the tip of the tentacles to the brain and beyond. Microscopy research and technique 24, 214-230.

Christian, K.A., Webb, J.K., Schultz, T.J., 2003. Energetics of bluetongue lizards (*Tiliqua scincoides*) in a seasonal tropical environment. Oecologia 136, 515-523.

Clarke, I.J., Sari, I.P., Qi, Y., Smith, J.T., Parkington, H.C., Ubuka, T., Iqbal, J., Li, Q., Tilbrook, A., Morgan, K., 2008. Potent action of RFamide-related peptide-3 on pituitary gonadotropes indicative of a hypophysiotropic role in the negative regulation of gonadotropin secretion. Endocrinology 149, 5811-5821.

Cropper, E.C., Miller, M.W., Tenenbaum, R., Kolks, M., Kupfermann, I., Weiss, K.R., 1988. Structure and action of buccalin: a modulatory neuropeptide localized to an identified small cardioactive peptide-containing cholinergic motor neuron of *Aplysia californica*. Proceedings of the National Academy of Sciences 85, 6177-6181.

Cummins, S.F., Tollenaere, A., Degnan, B.M., Croll, R.P., 2011. Molecular analysis of two FMRFamide-encoding transcripts expressed during the development of the tropical abalone *Haliotis asinina*. Journal of Comparative Neurology 519, 2043-2059.

Du, H., Bao, Z., Hou, R., Wang, S., Su, H., Yan, J., Tian, M., Li, Y., Wei, W., Lu, W., 2012. Transcriptome sequencing and characterization for the sea cucumber *Apostichopus japonicus* (Selenka, 1867). PloS one 7, e33311.

Firth, B.T., Christian, K.A., Belan, I., Kennaway, D.J., 2010. Melatonin rhythms in the Australian freshwater crocodile (*Crocodylus johnstoni*): a reptile lacking a pineal complex? Journal of Comparative Physiology B: Biochemical, Systemic, and Environmental Physiology 180, 67-72.

Fisher, J.M., Sossin, W., Newcomb, R., Scheller, R.H., 1988. Multiple neuropeptides derived from a common precursor are differentially packaged and transported. Cell 54, 813-822.

Furukawa, Y., Nakamaru, K., Wakayama, H., Fujisawa, Y., Minakata, H., Ohta, S., Morishita, F., Matsushima, O., Li, L., Romanova, E., 2001. The enterins: a novel family of neuropeptides isolated from the enteric nervous system and CNS of *Aplysia*. The Journal of Neuroscience 21, 8247-8261.

Guppy, M., Withers, P., 1999. Metabolic depression in animals: physiological perspectives and biochemical generalizations. Biological Reviews of the Cambridge Philosophical Society 74, 1-40.

Hahn, D.A., Denlinger, D.L., 2011. Energetics of insect diapause. Annu Rev Entomol 56, 103-121.

Hellen, C.U., Sarnow, P., 2001. Internal ribosome entry sites in eukaryotic mRNA molecules. Genes Dev 15, 1593-1612.

Hudson, N.J., Lonhienne, T.G.A., Franklin, C.E., Harper, G.S., Lehnert, S., 2008. Epigenetic silencers are enriched in dormant desert frog muscle. Journal of Comparative Physiology B: Biochemical, Systemic, and Environmental Physiology 178, 729-734.

Johannes, G., Sarnow, P., 1998. Cap-independent polysomal association of natural mRNAs encoding c-myc, BiP, and eIF4G conferred by internal ribosome entry sites. RNA 4, 1500-1513.

Lloyd, P., Mahon, A., Kupfermann, I., Cohen, J., Scheller, R., Weiss, K., 1985. Biochemical and immunocytological localization of molluscan small cardioactive peptides in the nervous system of *Aplysia californica*. The Journal of neuroscience 5, 1851-1861.

Lockyer, A.E., Spinks, J.N., Walker, A.J., Kane, R.A., Noble, L.R., Rollinson, D., Dias-Neto, E., Jones, C.S., 2007. *Biomphalaria glabrata* transcriptome: identification of cell-signalling, transcriptional control and immune-related genes from open reading frame expressed sequence tags (ORESTES). Developmental & Comparative Immunology 31, 763-782.

Mann, M., Jensen, O.N., 2003. Proteomic analysis of post-translational modifications. Nature biotechnology 21, 255-261.

Merkler, D.J., 1994. C-terminal amidated peptides: production by the in vitro enzymatic amidation of glycine-extended peptides and the importance of the amide to bioactivity. Enzyme and microbial technology 16, 450-456.

Miller, M., Alevizos, A., Cropper, E., Kupfermann, I., Weiss, K., 1992. Distribution of buccalin-like immunoreactivity in the central nervous system and peripheral tissues of *Aplysia californica*. Journal of Comparative Neurology 320, 182-195.
Miller, M., Beushausen, S., Cropper, E., Eisinger, K., Stamm, S., Vilim, F., Vitek, A., Zajc, A., Kupfermann, I., Brosius, J., 1993. The buccalin-related neuropeptides: isolation and characterization of an *Aplysia* cDNA clone encoding a family of peptide cotransmitters. The Journal of Neuroscience 13, 3346-3357.
Moroz, L.L., Edwards, J.R., Puthanveettil, S.V., Kohn, A.B., Ha, T., Heyland, A., Knudsen, B., Sahni, A., Yu, F., Liu, L., 2006. Neuronal transcriptome of *Aplysia*: neuronal compartments and circuitry. Cell 127, 1453-1467.
Norekian, T., Satterlie, R., 1997. Distribution of myomodulin-like and buccalin-like immunoreactivities in the central nervous system and peripheral tissues of the mollusc, *Clione limacina*. Journal of Comparative Neurology 381, 41-52.
Padilla, P.A., Ladage, M.L., 2012. Suspended animation, diapause and quiescence: arresting the cell cycle in *C. elegans*. Cell Cycle 11, 1672-1679.
Pirger, Z., Lubics, A., Reglodi, D., Laszlo, Z., Mark, L., Kiss, T., 2010. Mass spectrometric analysis of activity-dependent changes of neuropeptide profile in the snail, *Helix pomatia.* Neuropeptides 44, 475-483.
Ramnanan, C.J., Allan, M.E., Groom, A.G., Storey, K.B., 2009. Regulation of global protein translation and protein degradation in aerobic dormancy. Molecular and Cellular Biochemistry 323, 9-20.
Ramnanan, C.J., Storey, K.B., 2006. Suppression of Na+/K+-ATPase activity during estivation in the land snail *Otala lactea*. The Journal of Experimental Biology 209, 677-688.
Ramnanan, C.J., Storey, K.B., 2008. The regulation of thapsigargin-sensitive sarcoendoplasmic reticulum Ca(2+)-ATPase activity in estivation. Journal of comparative physiology. B, Biochemical, systemic, and environmental physiology 178, 33-45.
Raymond, J.L., Schulman, E.E., Baxter, D.A., Cleary, L.J., Byrne, J.H., 1989. Differential effects of the peptide buccalin and serotonin on membrane currents, action potential duration and excitability in pleural sensory neurons of *Aplysia*, Sot Neurosci Abstr, p. 1284.
Reilly, B.D., Schlipalius, D.I., Cramp, R.L., Ebert, P.R., Franklin, C.E., 2013. Frogs and estivation: transcriptional insights into metabolism and cell survival in a natural model of extended muscle disuse. Physiol Genomics 45, 377-388.
Ren, J., Wen, L., Gao, X., Jin, C., Xue, Y., Yao, X., 2009. DOG 1.0: illustrator of protein domain structures. Cell research 19, 271-273.
Rosen, S.C., Susswein, A.J., Cropper, E.C., Weiss, K.R., Kupfermann, I., 1989. Selective modulation of spike duration by serotonin and the neuropeptides, FMRFamide, SCPB, buccalin and myomodulin in different classes of mechanoafferent neurons in the cerebral ganglion of *Aplysia*. The Journal of Neuroscience 9, 390-402.
Santama, N., Wheeler, C.H., Burke, J.F., Benjamin, P.R., 1994. Neuropeptides myomodulin, small cardioactive peptide, and buccalin in the central nervous system of *Lymnaea stagnalis*: purification, immunoreactivity, and artifacts. Journal of Comparative Neurology 342, 335-351.
Steffensen, I., Syed, N., Lukowiak, K., Bulloch, A., Morris, C., 1995. Sensorin-A immunocytochemistry reveals putative mechanosensory neurons in *Lymnaea* CNS. Invertebrate Neuroscience 1, 207-213.
Stewart, M.J., Favrel, P., Rotgans, B., Wang, T., Zhao, M., Sohail, M., Wayne, A., Elizur, A., Henry, J., Cummins, S.F., 2014. Neuropeptides encoded by the genomes of the Akoya pearl oyster *Pinctata fucata* and Pacific oyster *Crassostrea gigas*: a bioinformatic and peptidomic survey. BMC genomics 15, 840.
Storey, K.B., 2002. Life in the slow lane: molecular mechanisms of estivation. Comparative Biochemistry and Physiology - Part A: Molecular & Amp; Integrative Physiology 133, 733-754.
Storey, K.B., Storey, J.M., 1990. Metabolic rate depression and biochemical adaptation in anaerobiosis, hibernation and estivation. The Quarterly review of biology 65, 145-174.
Storey, K.B., Storey, J.M., 2004. Metabolic rate depression in animals: transcriptional and translational controls. Biological Reviews 79, 207-233.
Storey, K.B., Storey, J.M., 2010. Metabolic regulation and gene expression during aestivation. Aestivation, 25-45.
Storey, K.B., Storey, J.M., 2012. Aestivation: signaling and hypometabolism. The Journal of Experimental Biology 215, 1425-1433.
Sweedler, J.V., Li, L., Rubakhin, S.S., Alexeeva, V., Dembrow, N.C., Dowling, O., Jing, J., Weiss, K.R., Vilim, F.S., 2002. Identification and characterization of the feeding circuit-activating peptides, a novel neuropeptide family of *Aplysia*. The Journal of Neuroscience 22, 7797-7808.
Syed, N., Bulloch, A., Lukowiak, K., 1990. *In vitro* reconstruction of the respiratory central pattern generator of the mollusk *Lymnaea*. Science 250, 282-285.
Tamura, K., Peterson, D., Peterson, N., Stecher, G., Nei, M., Kumar, S., 2011. MEGA5: molecular evolutionary genetics analysis using maximum likelihood, evolutionary distance, and maximum parsimony methods. Molecular biology and evolution 28, 2731-2739.

Veenstra, J.A., 2010. Neurohormones and neuropeptides encoded by the genome of *Lottia gigantea*, with reference to other mollusks and insects. General and Comparative Endocrinology 167, 86-103.
Vilim, F.S., Cropper, E.C., Rosen, S.C., Tenenbaum, R., Kupfermann, I., Weiss, K.R., 1994. Structure, localization, and action of buccalin B: a bioactive peptide from *Aplysia*. Peptides 15, 959-969.
Weiss, K.R., Bayley, H., Lloyd, P.E., Tenenbaum, R., Kolks, M.A., Buck, L., Cropper, E.C., Rosen, S.C., Kupfermann, I., 1989. Purification and sequencing of neuropeptides contained in neuron R15 of *Aplysia californica*. Proceedings of the National Academy of Sciences 86, 2913-2917.
Weiss, K.R., Cropper, E.C., Tenenbaum, R., Vilim, F.S., Kupfermann, I., 1988. Action and structure of parabuccalin—A novel neuropeptide localized to cholinergic buccal motoneurons B15 and B16 of *Aplysia*, Soc. Neurosci. Abstr., p. 177.
Winne, C.T., Willson, J.D., Gibbons, J.W., 2006. Income breeding allows an aquatic snake *Seminatrix pygaea* to reproduce normally following prolonged drought-induced aestivation. Journal of Animal Ecology 75, 1352-1360.

Figure legends

Figure 1. Investigation of the *T. pisana* CNS. (A) Whole-mount image of CNS. (B) Representative histological section of CNS with haematoxylin and eosin stain. (C) Schematic representation of CNS. CG, cerebral ganglia; CC, cerebral commissure; DBa, dorsal body area; LPaG, left parietal ganglia; RPaG, right parietal ganglia; PeG, pedal ganglia; LPlG, left pleural ganglia; RPlG, right pleural ganglia; PC, procerebrum; St, statocyst; TNv, tentacle nerve; MtC, metacerebrum; PCN, procerebrum.

Figure 2. Workflow for the identification of aestivation-associated peptides. *T. pisana* CNS peptides from active and aestivated snails were extracted and purified by nanoHPLC-MS/MS for determination of differential expression of peptides. The protein database was provided from a CNS-derived transcriptome obtained from pooled RNA from active and aestivated *T. pisana* (Adamson et al., 2015b).

Figure 3. Hierarchical clustering of peptides relative expression levels in the *T. pisana* CNS of aestivated versus active snails based on MS/MS analysis. The 19 differentially expressed peptides can be divided into two clusters. Names and further information about these peptides can be found in **Table 1**.

Figure 4. Analysis of the *T. pisana* buccalins. (A) Schematic representation of known buccalin precursor organisation in molluscs compared with a buccalin-like precursor of *Stegodyphus mimosarum*. (B) Multiple sequence alignment of Tpi-buccalin precursors. Blue shading shows amino acids that are highly conserved. Sequence log above alignment shows amino acid conservation, represented by letter size. MS/MS peptides identified are shown as red overline for buccalin-1 and green underline for buccalin-2. (C) Phylogenetic tree of mollusc buccalin precursors. *S. mimosarum* was used as an outgroup. Bootstrap values are shown and scale bar represents amino acid differences. All sequences used for analysis can be found in **File S1**. (D) Quantitative PCR expression analysis of Tpi-buccalin-2 in CNS of active and aestivated *T. pisana*.

Figure 5. *In situ* hybridisation analysis of *T pisana buccalin-2* in the aestivated CNS. (A) Control using sense DIG-labelled *buccalin-2* riboprobe. (B) Section showing positive staining using antisense DIG-labelled *buccalin-2* riboprobe. Regions boxed as (C-G) are shown magnified. CG, cerebral ganglia; DBa,

dorsal body area; meso, mesocerebrum; meta, metacerebrum; pro, procerebrum; PeG, pedal ganglia; PlG, pleural ganglia; VG, visceral ganglia.

Figure 6. Immunolocalisation analysis of *T. pisana* buccalin R_{102}LDKFGFSGGI-amide. (A-L) Localisation of peptide within sections of the aestivated CNS. PaG, parietal ganglia; PeG, pedal ganglia; PlG, pleural ganglia Further immunolocalisation is shown in **Figure S2**.

Additional files

File S1. List of all protein sequences used in this study.

Figure S1. Histological sections through the *T. pisana* CNS and stained haematoxylin and eosin. Serial sections are numbered 1-20.

Figure S2. Immunolocalisation analysis of aestivating *T. pisana* buccalin R_{102}LDKFGFSGGI-amide. Serial sections are numbered 1-24.

Figure S3. Immunolocalisation analysis of active *T. pisana* buccalin R_{102}LDKFGFSGGI-amide. Serial sections are numbered 1-11.

Table 1. List of peptides up- and down-regulated between active and aestivated *T. pisana* CNS.

Peptide name	Predicted avg mass	m/z	z (charge)	Aestivated	Active	Ratio	Sequence	Precursor length AA
Tpi-FCAP	1312.41	656.82	2	2.60E+04	0	1.00:0	GLDSLGGSQVHGW	173 (not FL)
	1388.50	694.8379	2	3.06E+04	2.57E+03	1.00:0.08	GLDSLGGYQVHGW	
Tpi-LFRF	1465.42	733.27	2	0	3.68E+03	00:01.0	SDSAQNPMDNEEE	155 (not FL)
Tpi-buccalin-1	1154.29	577.80	2	2.69E+04	9.98E+02	1.00:0.04	RLDSYGFAGGI	265
Tpi-buccalin-2	1165.36	583.33	2	6.29E+04	1.01E+04	1.00:0.16	RVDKFGFAGGI	277
	1195.39	598.33	2	2.68E+04	3.75E+03	1.00:0.14	RLDKFGFSGGI	
	1259.38	630.33	2	1.09E+04	1.53E+03	1.00:0.14	SRDNIGLSGLLD	
	1266.42	633.83	2	2.03E+04	7.79E+03	1.00:0.38	ELDPYGFSARI-amide(-.98)	
Tpi-enterin	960.06	480.74	2	6.35E+03	6.49E+02	1.00:0.10	GPNFGHSFV-amide(-.98)	279 (not FL)
Tpi-sCAP	1040.25	520.77	2	6.26E+03	1.57E+02	1.00:0.03	SGYLAFPRM-amide(-.98)	136
Tpi-pleurin	1474.64	492.26	3	8.78E+03	0	1.00:0	GVFTQGAHGSYPRV-amide(-.98)	179
	1595.78	797.91	2	4.01E+03	1.43E+03	1.00:0.36	TFYTGGNGIHYPRI-amide(-.98)	
Tpi-sensorin-A	1133.38	567.30	2	7.62E+03	0	1.00:0	AKYRVGYMF-amide(-.98)	110
Tpi-LASGLV_like	977.46	489.24	2	6.31E+03	0	1.00:0	RPFDELGSG	368 (not FL)
Tpi-AAP1	980.09	490.27	2	4.49E+03	0	1.00:0	GSQSSFVRI-amide(-.98)	408
Tpi-AAP2	2269.58	757.07	3	5.21E+03	0	1.00:0	SLEAALRAPPSIYSEALIEAPA	108
Tpi-AAP6	1699.88	567.29	3	3.52E+03	0	1.00:0	EEAASVKKETIHTEK	689 (not FL)
Tpi-AAP4	1106.31	369.20	3	4.41E+03	3.04E+01	1.00:0.01	RMHNFVRF-amide(-.98)	234
Tpi-AAP5	1117.32	373.20	3	7.40E+03	3.27E+02	1.00:0.04	AHHIGLGTALK	384 (not FL)
Tpi-AAP3	1936.02	645.97	3	5.57E+03	3.76E+02	1.00:0.07	FHYGLTKPEESSSNPGAD	486
Tpi-AAP8	1494.68	747.85	2	1.43E+05	2.99E+04	1.00:0.21	IMDSLSSADTVTVR	103 (not FL)
Tpi-AAP7	1496.6	748.37	2	4.42E+03	1.11E+03	1.00:0.25	RFDSISGHSSFGSL	431 (not FL)
Tpi-AAP9	1172.41	396.89	3	6.31E+02	0	1.00:0	GVM(+15.99)GKSAGQLPK	205
Tpi-AAP14	1863.95	621.98	3	4.40E+02	1.90E+03	1.00:4.31	AKAVSGDAVESGSKTEDVN	211 (not FL)

m/z, mass to charge; FL, full-length

Table 2. List of abundance of differentially expressed gene transcripts of peptides in CNS, hepatopancreas and muscle tissue in *Theba pisana*.

Name	Peptides	Peptide sequence	CNS		Hepatopancreas		Muscle	
			FPKM	Rank/250849	FPKM	Rank/250849	FPKM	Rank/250849
Tpi-FCAP	**2**	GLDSLGGSQVHGW, GLDSLGGYQVHGW	24	5282	0	248825	0.82	135316
Tpi-LFRF	**1**	SDSAQNPMDNEEE	454	268	0.07	200159	140.1	693
Tpi-buccalin-1	**1**	RLDSYGFAGGI	2	74800	0	212103	0.11	202414
Tpi-buccalin-2	**5**	RVDKFGF, RVDKFGFAGGI, RLDKFGFSGGI, SRDNIGLSGLLD, ELDPYGFSARI(-.98)	2785	14	1.59	82660	8.3	18598
Tpi-enterin	**1**	GPNFGHSFV(-.98)	679	174	22.43	5301	109.91	907
Tpi-sCAP	**1**	SGYLAFPRM(-.98)	732	157	0.32	166885	0.2	189403
Tpi-pleurin	**3**	GVFTQGAHGSYPRV(-.98), GVFTQGAHGSYPRV(-.98), TFYTGGNGIHYPRI(-.98)	727	159	0.52	149226	1.8	82235
Tpi-sensorin-A	**1**	AKYRVGYMF(-.98)	55	2244	0	211611	7	22454
Tpi-LASGLV like	**1**	RPFDELGSG	108	1134	10	12935	20.15	6602
Tpi-AAP1	**1**	GSQSSFVRI(-.98)	54	2264	0.05	202979	3.58	44600
Tpi-AAP2	**1**	SLEAALRAPPSIYSEALIEAPA	470	252	0.94	118491	2.4	64478
Tpi-AAP6	**1**	EEAASVKKETIHTEK	0.13	196410	0.92	119893	3.65	43808
Tpi-AAP4	**1**	RMHNFVRF(-.98)	67	1823	1.09	108866	24.22	5275
Tpi-AAP5	**1**	AHHIGLGTALK	2.7	55715	10.83	4339	97.83	1041
Tpi-AAP3	**1**	FHYGLTKPEESSSNPGAD	6	24113	0.01	204664	0.9	130035
Tpi-AAP8	**1**	IMDSLSSADTVTVR	2	75851	0.09	197956	0	236945
Tpi-AAP7	**1**	RFDSISGHSSFGSL	54	2279	0.09	198107	1.64	88434
Tpi-AAP9	**2**	GVM(+15.99)GKSAGQLPK, GVMGKSAGQLPK	569	211	0.67	137337	4.63	34607
Tpi-AAP14	**1**	AKAVSGDAVESGSKTEDVN	18	7181	0	205757	3.91	40979

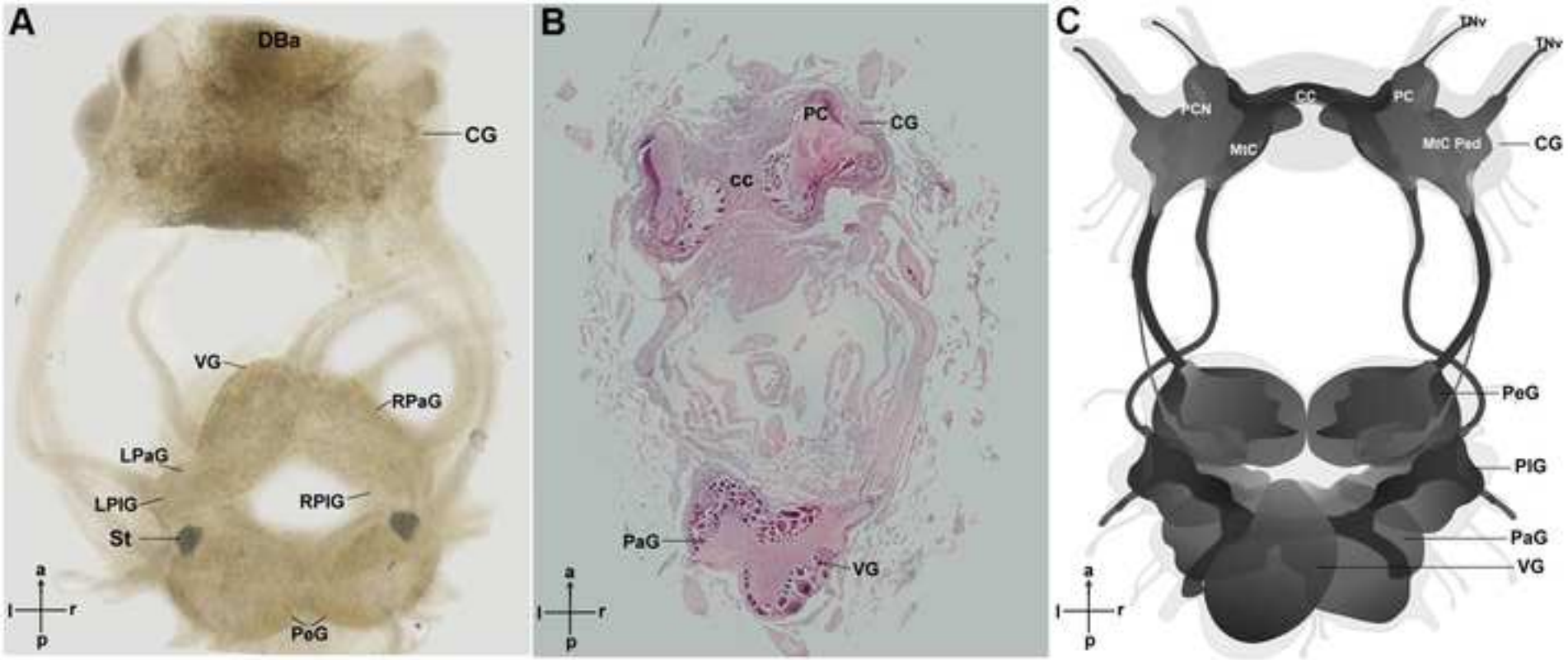

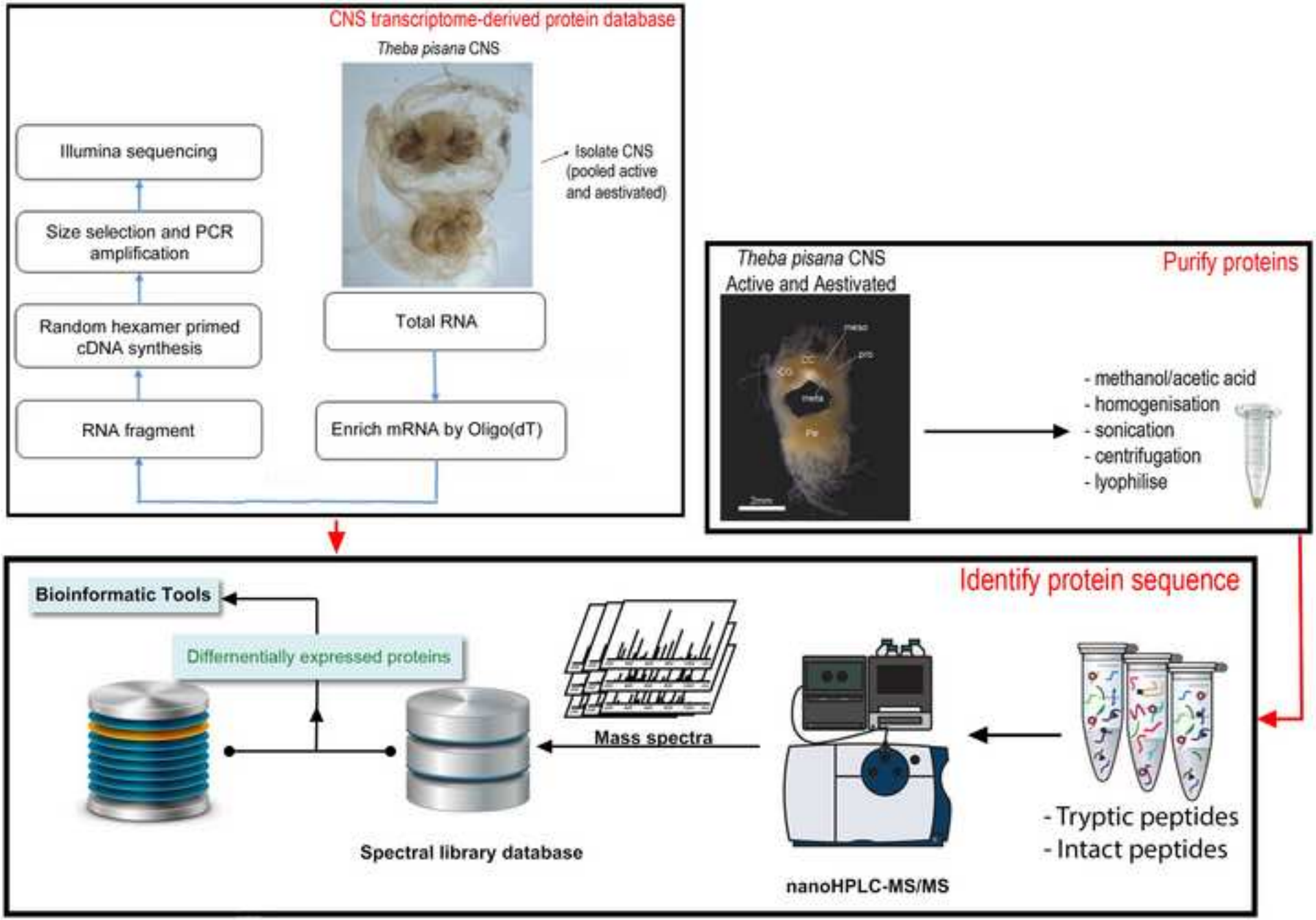

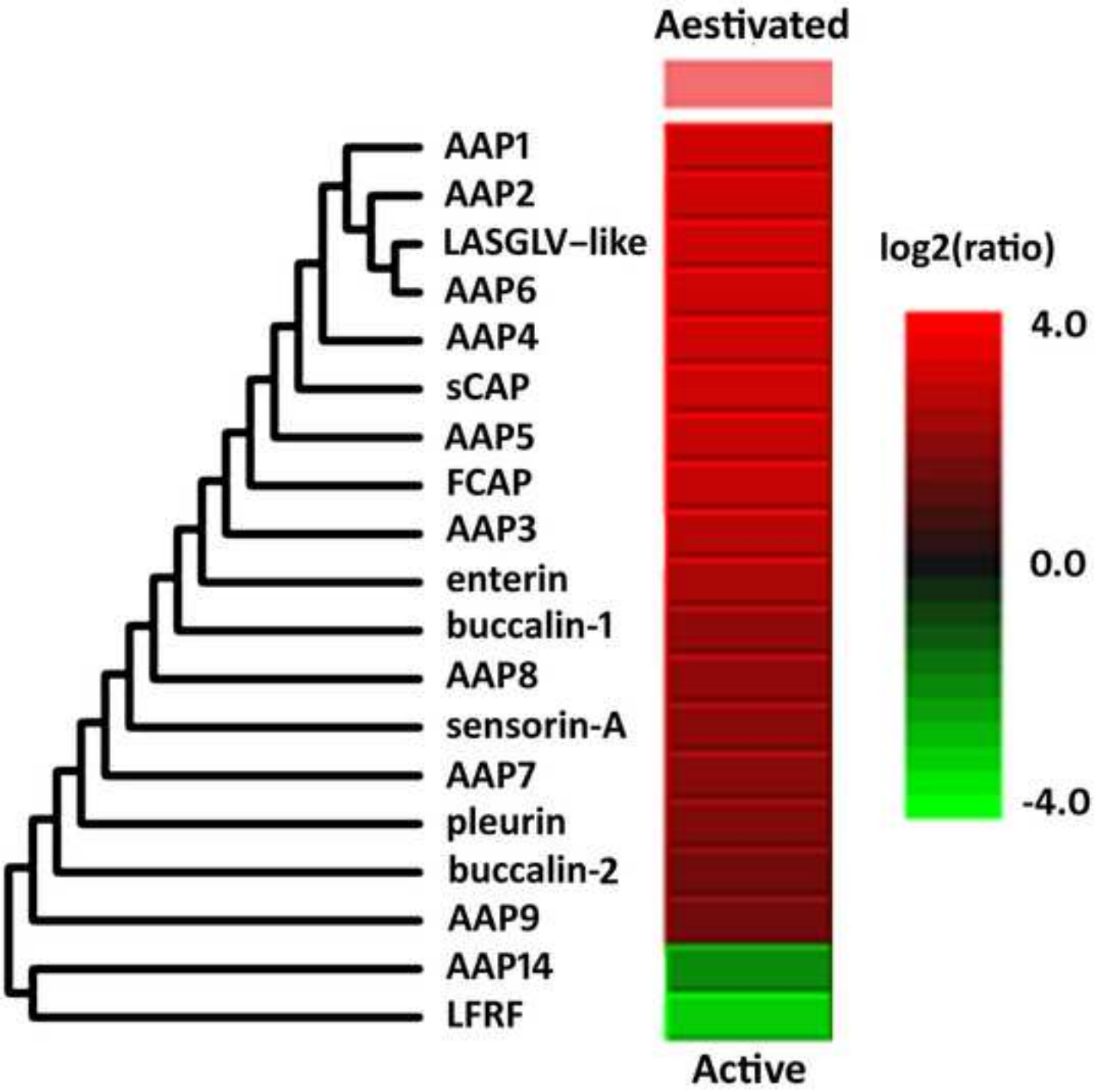
Aestivated
AAP1
AAP2
LASGLV–like
AAP6
AAP4
sCAP
AAP5
FCAP
AAP3
enterin
buccalin-1
AAP8
sensorin-A
AAP7
pleurin
buccalin-2
AAP9
AAP14
LFRF
Active
log2(ratio)
4.0
0.0
-4.0

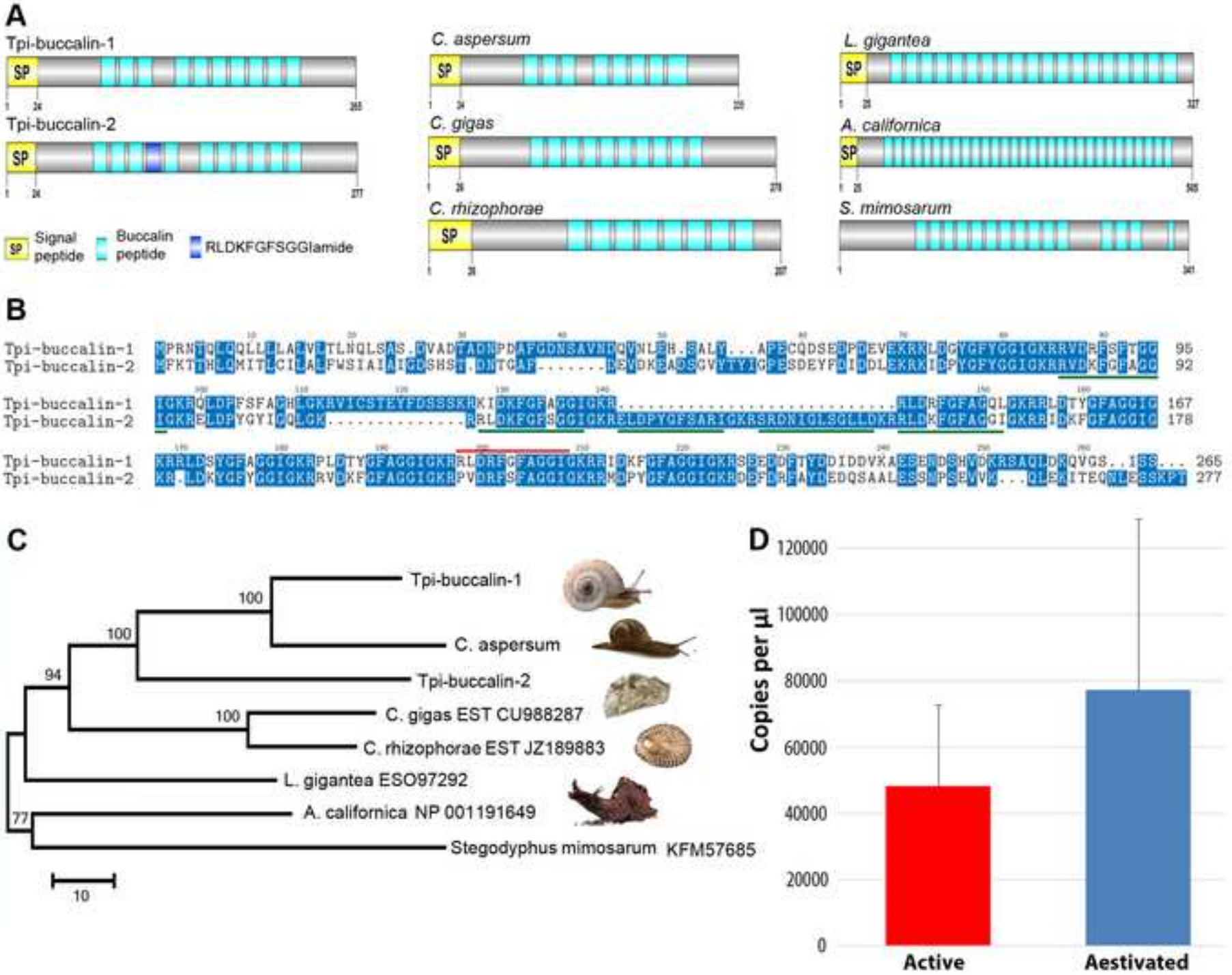

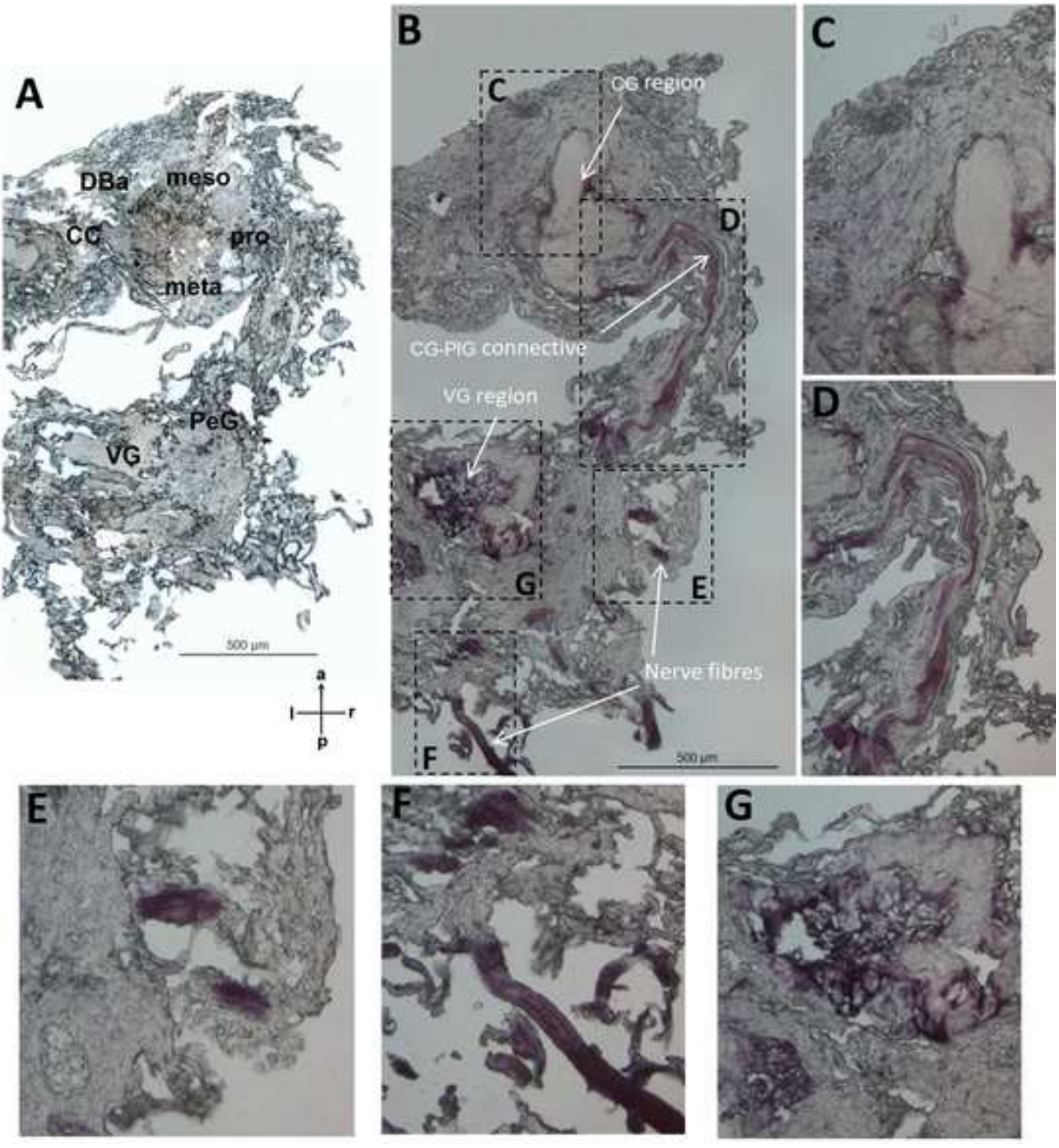

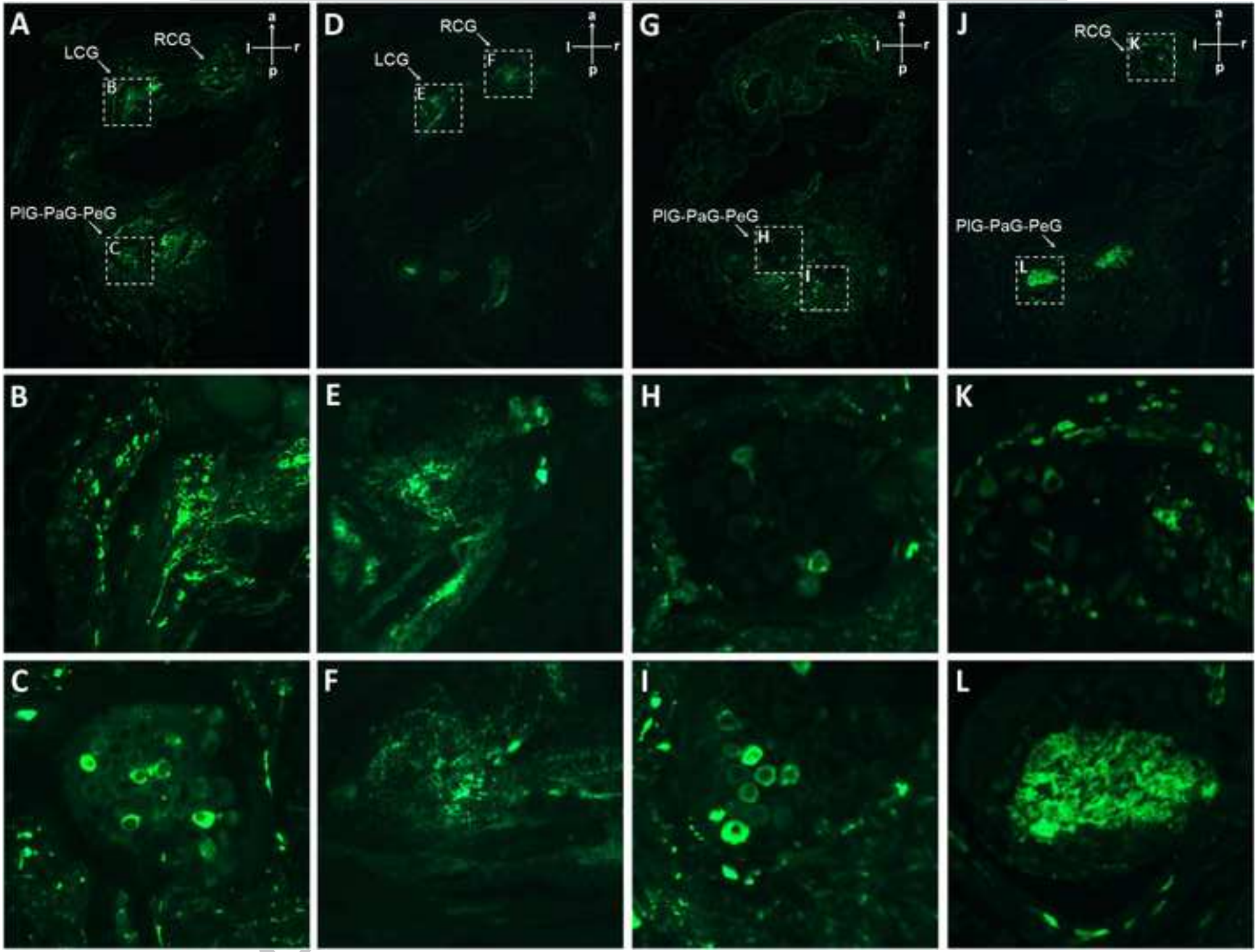

- Aestivation alters *Theba pisana* CNS peptide abundance.
- The buccalin neuropeptide is upregulated in aestivation CNS
- Four *buccalin* gene transcripts are capable of producing numerous buccalin peptides
- Buccalin is widespread throughout the CNS regions